Self-organization of bacterial biofilms is facilitated by extracellular DNA

Erin S. Gloag[a,1], Lynne Turnbull[a,1], Alan Huang[b], Pascal Vallotton[c], Huabin Wang[d], Laura M. Nolan[a], Lisa Millili[e], Cameron Hunt[e], Jing Lu[a], Sarah R. Osvath[a], Leigh G. Monahan[a], Rosalia Cavaliere[a], Ian G. Charles[a], Matt P. Wand[b], Michelle L. Gee[d], Ranganathan Prabhakar[e] and Cynthia B. Whitchurch[a,2]

[a]The ithree institute, University of Technology Sydney, Ultimo, NSW, 2007, Australia.

[b]School of Mathematics, University of Technology Sydney, Ultimo, NSW, 2007, Australia.

[c]CSIRO Mathematics, Informatics and Statistics, North Ryde, NSW, 1670, Australia.

[d]School of Chemistry, The University of Melbourne, Parkville, VIC, 3010, Australia.

[e]Department of Mechanical & Aerospace Engineering, Monash University, Clayton, VIC, 3800, Australia.

[1] These authors contributed equally to this work.

[2]Correspondence to: Cynthia Whitchurch

PO Box 123, Broadway NSW 2007, Australia

+61 2 9514 4144

Cynthia.Whitchurch@uts.edu.au

Classification: BIOLOGICAL SCIENCES: Microbiology

Keywords: twitching motility, eDNA, t4p, type IV pili, collective behaviour

Abstract

Twitching motility mediated biofilm expansion is a complex, multicellular behavior that enables the active colonisation of surfaces by many species of bacteria. In this study we have explored the emergence of intricate network patterns of interconnected trails that form in actively expanding biofilms of *Pseudomonas aeruginosa*. We have used high resolution phase contrast time-lapse microscopy and developed sophisticated computer vision algorithms to track and analyse individual cell movements during expansion of *P. aeruginosa* biofilms. We have also used atomic force microscopy to examine the topography of the substrate underneath the expanding biofilm. Our analyses reveal that at the leading edge of the biofilm, highly coherent groups of bacteria migrate across the surface of the semi-solid media, and in doing so, create furrows along which following cells preferentially migrate. This leads to the emergence of a network of trails that guide mass transit toward the leading edges of the biofilm. We have also determined that extracellular DNA (eDNA) facilitates efficient traffic flow throughout the furrow network by maintaining coherent cell alignments, thereby avoiding traffic jams and ensuring an efficient supply of cells to the migrating front. Our analyses reveal that eDNA also co-ordinates the movements of cells in the leading edge vanguard rafts and is required for the assembly of cells into the "bulldozer" aggregates that forge the interconnecting furrows. Our observations have revealed that large-scale self-organization of cells in actively expanding biofilms of *P. aeruginosa* occurs through construction of an intricate network of furrows that is facilitated by eDNA.

body

Introduction

Bacterial biofilms are multicellular communities of bacteria that are embedded in a self-produced polymeric matrix comprised of polysaccharides, proteins and extracellular DNA (eDNA). Biofilms are prevalent in nature as well as in industrial and medical settings, where colonization of new territories by bacteria can occur via active biofilm expansion, leading to biofouling of marine and industrial surfaces, and the spread of infection within host tissues and along implanted medical devices (1-3).

When cultured on the surface of solidified nutrient media, many bacteria are able to actively expand their colony biofilms through co-ordinated motions that can be powered by different mechanisms including flagella rotation, type IV pili (tfp) retraction and/or slime secretion. The soil organism *Myxococcus xanthus* actively swarms away from the point of inoculation through a process termed gliding motility which is mediated by two types of motility: A motility which occurs through an unknown mechanism and S motility which is powered by tfp retraction (4, 5). *M. xanthus* swarming is a complex multicellular process that has been extensively studied and in recent years a number of mathematical models have been developed to describe this behavior (6-9).

Twitching motility is a mechanism of surface translocation that has been observed in many species of bacteria (10) and is closely related to S motility of *M. xanthus*. These motilities are both powered by the extension, surface binding and retraction of tfp located at the leading edge pole of the cell resulting in translocation of an individual bacterial cell (11, 12). We have observed previously that when the opportunistic pathogen *Pseudomonas aeruginosa* is cultured at the interface of solidified nutrient media and a glass coverslip, the biofilms that

form in the interstitial space expand rapidly via twitching motility and can form a vast, intricate network of interconnected trails (13). Interstitial biofilm expansion by *P. aeruginosa* appears to be a highly organised multicellular behavior that arises through the collective co-ordination of individual cellular movements involving the migration of rafts of cells at the leading edge of the biofilm that appear to lay down a trail of unknown composition along which cells preferentially migrate (13). The mechanisms involved in co-ordinating individual activities during this complex multicellular behavior or that lead to the formation of the dramatic interconnected trail network in *P. aeruginosa* biofilms are currently unknown.

The emergence of self-organized patterns in living and non-living systems has fascinated scientists for centuries and there is widespread interest in understanding the mechanisms behind these (14). Common features displayed by these self-organized phenomena are the formation of trails that lead to the emergence of dramatic patterns of large-scale order (15). The processes leading to pattern formation in biological systems are likely to be more complex than the spontaneous emergence of patterns that are observed in non-living systems and will involve an interplay of physical, chemical and biological parameters (16, 17).

Multicellular behaviors in bacteria are often controlled via chemical signaling systems such as quorum sensing (18). However, we have shown previously that twitching motility mediated biofilm expansion by *P. aeruginosa* is not controlled through quorum sensing (19). Interestingly, the exopolysaccharide slimes which are produced during gliding and flagella-dependent swarming motilities are visualised microscopically as phase bright trails. These slime trails are laid down by cells as they migrate across the surface and direct cellular movements of following cells (20, 21). In *M. xanthus*, tfp have also been shown to bind to the polysaccharide component of extracellular fibrils located on the surface of neighboring cells.

The production of fibrils is essential for S motility in *M. xanthus* where it is thought that the polysaccharide component provides an optimal surface for tfp binding, inducing retraction of the filament and subsequent translocation of the cell (22). It has not yet been determined if an extracellular slime similarly contributes to *P. aeruginosa* twitching motility mediated biofilm expansion.

Results

Quantitative analysis of cell movements during interstitial biofilm expansion.

We have developed a model system to study interstitial biofilm expansion by *P. aeruginosa*, in which the interstitial biofilm expands via twitching motility as a monolayer. This model enables visualization of individual cells in the biofilm using high resolution phase contrast microscopy which avoids potential photo-toxicity artifacts that can be associated with the use of fluorescence microscopy. Time series of *P. aeruginosa* intersititial biofilm expansion were captured at 1 frame /2 s. Visual inspection of 1000 frame time-series (2000 s) shows that biofilm expansion involves an almost constant streaming of cells that migrate from the main biofilm along the trail network into rafts of cells at the leading edge (Video S1). Cells behind the leading edge are tightly aligned in narrow intersecting trails with the major cell axes oriented along the overall direction of the trail in which they were moving. Cells within these trails appear to be in relatively constant motion with the overall direction of movement toward the leading edge (Videos S1).

To enable quantitative analyses of individual cellular movements during biofilm expansion, we have developed an automated cell tracking algorithm to identify and track the movements of all individual bacterial cells present in the field of view across consecutive frames (see Supplementary Information; (23, 24)). Whilst individual bacteria can be distinguished clearly

by human vision in our interstitial biofilm images (Fig 1A, C, S1A), obtaining their precise outlines using computer vision is relatively challenging. We therefore developed sophisticated computer vision methods to identify and track individual bacteria (see Supplementary Information; (23, 24)).

Quantitative analysis of the data obtained from the cell tracking was utilised to examine the cell movements during 100 s of interstitial biofilm expansion by *P. aeruginosa* (Fig 1A-D). Cells were separated into three populations based on their location within the biofilm. Cells within the leading edge vanguard rafts are referred to as "raft head", cells within the trail immediately behind the raft as "raft trails" and cells within the trail network as "behind the leading edge" (Fig 1A, C). Our quantitative analyses indicate that cells within the raft head tend to be highly aligned along the longitudinal axis of the cell (orientational coherence, Fig S2) and to move in the same direction as their neighbors (velocity coherence) (Fig 2A). Cells in raft trails and behind the leading edge, however, have reduced orientation and velocity coherence with their neighbors indicating that these cells tend to move more independently of their nearest neighbours (Figs 2A, S2).

Analysis of the distance travelled by individual cells in 100s reveals that cells within the raft head, raft trails and behind the leading edge travel at similar total distances with median values of 5.77, 5.93 and 5.86 μm respectively (Fig 2B). However, the net displacements of the cells in these regions showed median values of 4.70, 1.95 and 2.56 μm respectively (Fig 2C). These analyses indicate that cells within the raft head undergo few directional changes whereas cells located within the raft trails and behind the leading edge show more frequent directional changes, which accounts for the reduced correlation between total and net distances travelled. Analyses of time-decays of orientation and velocity direction

autocorrelations confirm that cells in the raft head tend to maintain their orientation and direction of travel whereas cells in the trails tend to change their orientation and direction of travel more frequently (Fig 2D, S2).

Our visual observations of extended (2000 s) time-series suggest that there is a relatively constant stream of cells moving through the trails toward the leading edge. To explore this further, the distances travelled across 2s intervals (frame to frame) were analysed. These analyses reveal that in any given 2s interval approximately 55% of cells in the raft head, 50% within the raft trails and 40% behind the leading edge traverse distances between 0.1 - 1.3 μm with the majority of these motile cells travelling between 0.1 – 0.4 μm / 2 s (Fig S3A).

Interestingly, *M. xanthus* cells also frequently change the direction of motion during swarm expansion. Mathematical modeling of *M. xanthus* swarming has suggested that cellular reversals enable a steady supply of cells to the advancing edge of the swarm by preventing traffic jams that form as a result of cellular collisions. (6, 7). We propose that the changes in direction of motion displayed by *P. aeruginosa* cells within the trail network could similarly enable efficient flow of cells through the biofilm to supply the advancing edge. Once at the outer edge, cells within the advancing raft heads maintain high velocity coherence with their neighbors and exhibit few directional changes as they colonise new territories.

Twitching motility mediated biofilm expansion involves the formation of a network of interconnected furrows

Our observations indicate that during interstitial biofilm expansion cells appear to be confined to trails of an unknown nature (Video S1). We have found that similar to our observations of interstitial biofilm expansion, twitching motility mediated expansion of the

colony biofilm also involves the migration of aggregates of cells at the leading edge that venture into unoccupied territories. Interestingly, migration of these vanguard groups creates a phase-bright trail along which following cells are able to migrate individually or in small groups but remain confined to the trail (Fig 3A, Video S2). These phase-bright trails are very similar in appearance to the slime trails that are produced during gliding or flagella-dependent swarming motilities (20, 21). Indeed the edges of the expanding *P. aeruginosa* colony biofilms (Fig 3A, S8C) bear a striking resemblance to *M. xanthus* swarms cultured on the surface of solidified growth media (25).

Our observations suggest that expansion of *P. aeruginosa* colony biofilms on the surface of solidified nutrient media is very similar to the expansion of interstitial biofilms. In light of the phase bright trails that we observed at the edges of the surface colony biofilms (Fig 3A), we hypothesised that a similar trail network may exist within interstitial biofilms. To explore this possibility, the media that supported the *P. aeruginosa* interstitial biofilms was imaged by phase-contrast microscopy (Fig 3C). This revealed that the substrate beneath the biofilm contained a series of interconnecting phase-bright trails, that directly correspond to the network of cells that comprised the biofilm prior to washing except at the leading edge where faint phase-bright trails can be seen directly in front of vanguard rafts of cells (Fig 3B-D). This is likely due to the continued forward migration of the rafts during the interval between imaging the intact biofilm and removal of the cells by washing.

Interestingly, we found that the phase-bright trails remain visible despite extensive washing. This suggests that the trails may not be comprised of a “slime” substance. We have noted that scratches in the media are phase-bright in appearance when visualised by phase-contrast microscopy and that *P. aeruginosa* cells that encounter the scratches tend to preferentially

migrate along them. We therefore considered the possibility that the trails that develop during *P. aeruginosa* biofilm expansion may be a consequence of physical furrows or grooves in the media that guide cell movement thereby leading to trail formation.

To determine if the phase-bright trails are physical furrows in the media, we used tapping mode Atomic Force Microscopy (AFM) to analyse the surface topography of the substrate beneath the biofilm which revealed the presence of numerous furrows that are consistent in dimension with the phase-bright trails observed in the interstitial biofilms (Figs 3E, F, S4-5; see Supplementary Information). Interestingly, AFM also showed that the furrows under the leading edge rafts are shallower than the trails and are comprised of ramps to the surface of the media (Fig. S6; see Supplementary Information). Phase-contrast imaging of washed biofilms shows that the front edge of the rafts tend to be less visible than the trails (Fig 3C) which is consistent with these being shallower than the trails. These observations suggest that the vanguard rafts migrate over the surface of the media and in the process plough a furrow into the media similar to the action of skis moving across snow.

Our observations suggest that the presence of an extensive furrow system accounts for the manifestation of the intricate trail network in *P. aeruginosa* biofilms as they actively expand over solidified nutrient media. To understand how the interconnected furrow system is forged, we used time-lapse microscopy to examine the process by which cells break out from the furrows to form intersecting trails (Fig 3G, Video S3). We analysed the formation of 26 interconnecting trails across 7 time-lapse series and observed that interconnecting trails are initiated by small groups comprised of on average 9.4 ± 2.4 cells (minimum 5; maximum 15; median 9) that become longitudinally aligned and oriented perpendicular to the trail. We found that these cells became stationary following re-alignment. The constant motion of cells

in the trail behind this initial cluster results in some cells coming into direct contact with these perpendicular cells and subsequently re-orienting so that a second layer, of an average of 9.5 ± 2.8 (minimum 4; maximum 17; median 10) longitudinally aligned cells form behind the initial cluster. Continued migration of cells behind this two layered cluster, results in more cells re-orienting with those within the expanding cluster until the supply of cells is sufficient for the newly formed aggregate to commence movement and break away from the trail edge (Fig 3G, Video S3). When an advancing raft connects with a neighboring raft or trail, the cells from the two paths merge together, resulting in the formation of the extensive trail network (Video S3). In light of the AFM data, these observations suggest that the co-ordinated action of an assembled aggregate with a constant supply of cells is required to breach the lip of the furrow in order to create a new furrow that then intersects with other furrows to form the intricate lattice-like network of trails. Our observations also suggest that a continuous supply of cells to these "bulldozer" aggregates is required to enable them to breach the lip of the furrow and to migrate into virgin territory.

Extracellular DNA facilitates twitching motility mediated biofim expansion

As biofilms of *P. aeruginosa* contain large quantities of eDNA (26-30) and the tfp of *P. aeruginosa* have been shown to bind DNA (31) we explored the possibility that eDNA may also contribute to the twitching motility mediated biofilm expansion. We have found that incorporation of the eDNA degrading enzyme DNaseI into the nutrient media significantly decreased twitching mediated expansion of *P. aeruginosa* colony biofilms by 76% (Supplementary Information, Fig S8). Fluorescence microscopy of interstitial biofilms cultured in the presence of the eDNA stain TOTO-1 revealed that these contain numerous bright punctate foci of eDNA from which tendrils of eDNA emanated, and that beyond these bright foci, eDNA is present at low levels throughout all areas of the interstitial biofilm (Fig

4A-E, Supplementary Information, Fig S8). Time-lapse imaging revealed that as a consequence of cells translocating through areas of high eDNA content, the eDNA becomes re-distributed within the biofilm, forming thin tendrils of eDNA radiating from the foci and aligned with the direction of cell migration (Fig 4E, Video S4). Interestingly, incorporation of DNaseI inhibited the formation of the intricate network of trails (Fig 1G, S8).

To explore the role of eDNA in *P. aeruginosa* biofilm expansion, time series of interstitial biofilm expansion in the presence of DNaseI were captured at 1 frame /2 s. Visual inspection of 1000 frame time-series showed that in the presence of DNaseI, cells at the leading edge were arranged in vanguard rafts that were similar in appearance to the rafts formed in the absence of DNaseI (Fig 1E, Video S5). However, in the presence of DNaseI the rafts showed very little outward migration compared to biofilms cultured in the absence of the enzyme (Video S5). Behind these rafts, cells were arranged haphazardly in broad paths fringed by stationary, laterally aligned cells that are oriented with their major axis perpendicular to the path (Figs 1G, S8G). Cells within the broad paths showed regions of densely packed misaligned cells that appeared to be caught in traffic jams and exhibited little to no movement, whereas in less dense areas individual cells were able to move (Fig 1H, Video S5).

To better understand the influence of DNaseI on biofilm expansion, cell movements in 100 s of the time-series were tracked (Fig 1F, H) and quantitatively analysed. These analyses revealed that the presence of DNaseI significantly reduced both the total and net distances translocated by individual cells in the expanding biofilm, compared to biofilms cultured in the absence of the enzyme (Fig 2B, C). Within the raft head, in the presence of DNaseI, cells displayed median total and net distances of 2.02 and 0.62 μm respectively, 1.96 and 0.46 μm

within the raft trails and 1.60 and 0.29 μm behind the leading edge (Fig 2B, C). We have further explored the impact of DNaseI on cell movements by comparing net displacements exhibited by the cells as a ratio of the total distance travelled in sub-groups of cells separated according to the total distances travelled when cultured in the presence or absence of DNaseI (Fig S3B). These analyses reveal that whilst DNaseI significantly reduces the distances traversed by the majority of cells, there remains a small proportion of cells that can travel considerable total distances. However, the presence of DNaseI significantly reduced the net displacements of these highly motile cells indicating that these cells often alter their direction of migration. Analyses of time-decays of orientation and velocity direction correlations confirm that in the presence of DNaseI, cells tended to frequently change their orientation and direction of travel (Figs 2D, S2B). Interestingly, in the presence of DNaseI, cells in all areas of the biofilm demonstrated very reduced values for both orientational coherence and velocity coherence indicating that these cells are moving independently of their nearest neighbours (Figs 2A, S2A). These analyses indicate that the presence of DNaseI results in a loss of co-ordinated behaviour during interstitial biofilm migration and that whilst most cells are non-motile in the presence of DNaseI, those cells that do move, tend to move independently of their neighbors and often alter their direction of motion.

To further understand the movements of the population of cells that are capable of migrating large total distances in the presence of DNaseI, the frame-to-frame movement (2 s intervals) of all cells over 100 s were examined. It is evident from these analyses that in the presence of DNaseI that approximately 90% of cells in both the leading edge and behind the leading edge, are almost completely stationary, travelling in any given 2 s < 0.1 μm (Fig S3A). However, in any 2 s, there is also a small proportion of cells that are capable to travelling up to 1.3 μm (Fig S3A). Interestingly, when the populations of cells that travel at distances > 0.6

μm in any 2s are looked at more closely, it is evident that the distribution of highly motile cells appears quite similar in both the presence and absence of DNaseI (Fig S3A) which suggests that eDNA likely does not necessarily act as a slippery "slime" to lubricate individual cell movements.

We have often observed in our time-lapse movies of interstitial biofilm expansion that when a raft separates from the biofilm its rate of migration slows, and at times ceases, until it is reconnected with a supply of cells from the biofilm. This suggests that a constant supply of cells to the outer edge of the expanding biofilm is required to maintain movement of the vanguard rafts as they translocate into virgin territory. In the presence of DNaseI, however, the supply of cells to the leading edge rafts from the biofilm is not continuous and can become completely inhibited by traffic jams caused by clusters of misaligned cells (Figs 1E, G, Video S5). The observed inhibition in the rate of migration of vanguard rafts in the presence of DNaseI may therefore be a consequence of inefficient supply of cells to the leading edge due to traffic jams throughout the biofilm.

In the presence of DNaseI, cells appear to be located within broad tracks edged by laterally aligned cells (Fig 1G). Phase contrast imaging of washed interstitial biofilms reveals the presence of broad phase-bright tracks that correspond to the populated regions of the biofilm (Fig 4F, G). AFM revealed that inclusion of DNaseI to the media produces broad furrows with high walls that are consistent with the phase-bright tracks (Fig 4H, I, S4-5; See Supplementary Information). AFM shows that in the presence of DNaseI, rafts are often situated within deep furrows with steep ramps to the surface (Figs 4F, S6C; See Supplementary Information). Interestingly, we observed that when cells in interstitial biofilms were killed with paraformaldehyde prior to washing and imaging by AFM, that the

ramps to the surface were no longer present and instead it appeared as if the rafts had sunk into the media and were surrounded by steep walls (Fig S6E, F). Our AFM data, taken together with our detailed analyses of cell movements, suggest that eDNA serves to direct traffic flow throughout the furrow network to efficiently supply cells to the leading edge rafts in order for them to attain sufficient speed to skim across the surface and avoid sinking into the semi-solid media.

Visual inspection of extended (2000 s) time-series of interstitial biofilm expansion in the presence of DNaseI reveals that whilst cells are aligned laterally in fringes at the edges of the paths, groups of longitudinally aligned cells do not assemble behind these lateral edge cells (Video S5). Thus eDNA appears to be required for the construction of interconnecting trails by co-ordinating both the assembly and supply of cells to "bulldozer" aggregates.

In summary the inclusion of DNaseI significantly inhibits the traffic flow of cells through the biofilm, characterised by a significant proportion of cells being almost completely stationary at any given time and a lack of coordinated movement of the remaining cells that were capable of some motion. The observed inhibition in the rate of migration of the vanguard rafts in the presence of DNaseI may therefore be a consequence of inefficient supply of cells to the leading edge due to traffic jams throughout the biofilm (Video S5) which is further exacerbated by the tendency of the slow moving aggregates to sink into the media rather than skimming across the surface. Thus it is evident that eDNA is required for coordinating the mass transit of cells through the biofilm for efficient supply of cells into the advancing edge and maintaining collective behaviors, particularly within the vanguard rafts.

Interestingly, interstitial biofilms of non-typeable *Haemophilus influenzae* and *Acinetobacter baumanii* which also actively expand via twitching motility (32, 33) are not associated with the formation of intricate network patterns of trails despite the presence of eDNA in these biofilms (Fig S9). This suggests that pattern formation by *P. aeruginosa* involves other factors in addition to simply the capacity for twitching motility in the presence of eDNA. Both *H. influenzae* and *A. baumanii* are coccobacilli whereas *P. aeruginosa* cells are rods, thus it is possible that cell morphology impacts the tendency toward nematic alignment along the long axis leading to efficient movement of cells and the emergence of trails. Modeling of *M. xanthus* swarming indicates that the rod morphology of *M. xanthus* cells and regular reversals of movement influence the rate of swarm expansion by reducing the collisional cross-section and enabling escape from collisions and traffic jams (6, 7).

Discussion

Close-packing of rod-shaped anisotropic objects leads to nematic order in suspensions of self-propelled particles (active suspensions) (34). However, this alone does not account for the emergence of the intricate network of trails that forms in actively expanding *P. aeruginosa* interstitial biofilms. In this study, the use of sophisticated computer vision and cell tracking along with AFM, provided novel insights into the mechanisms that contribute to emergent pattern formation in biological systems. We have identified additional layers of complexity over the basic tendency for nematic alignment in dense collectives of rods. Firstly, there is the formation of the furrow network, which is a pattern more complex than a nematic liquid crystal. Our observations suggest that during interstitial biofilm expansion, the bacteria are tunneling through the interface between the glass substrate and the semi-solid media, and it is possible that the observed furrow network is an emergent consequence of the mechanical interactions between the self-propelled nematic liquid crystal pushing against the

soft gel, causing it to locally de-bond from the glass surface. Secondly, we have found that eDNA appears to be crucial in assembly and co-ordinating the collective behavior of cells in "bulldozer" rafts that forge the furrows as well as in preserving the integrity of the network structure once it has been formed. These physical mechanisms coupled with the active nematogenic behaviour of rod-shaped bacterial cells lead to the formation of dramatic interconnected network of trails during interstitial biofilm expansion by *P. aeruginosa*.

Our quantitative analyses of the tracking data reveals that eDNA serves to maintain constant traffic flow throughout the trail network by maintaining relative cell alignment. *P. aeruginosa* cells have been shown to spontaneously orient with the direction of extended, concentrated DNA molecules (35). Our time-lapse imaging of interstitial biofilm expansion in the presence of the eDNA stain TOTO-1 revealed that as cells migrated through areas of high eDNA content, they dragged the eDNA along causing it to be generally aligned with the direction of cell movement (Fig. 4C, Video S4). We propose that this process creates a bed of concentrated, aligned eDNA molecules within the furrow network that helps co-ordinate collective behaviours by enhancing nematic alignment.

It is evident from our fluorescence microscopy of TOTO-1 stained interstitial biofilms that whilst eDNA is not homogenously distributed throughout the biofilm, that all areas of the biofilm including the leading edge rafts contain eDNA. Our observations indicate that eDNA is important in co-ordinating bacterial movements during biofilm expansion and it is clear that inclusion of DNaseI dramatically alters cell behavior and inhibits biofilm expansion. Our analyses revealed that inclusion of DNaseI dramatically affects the behavior of cells predominantly in the leading edge raft heads causing them to lose coherence with their neighbours. These observations are consistent with a role for eDNA in also mediating

intercellular connectivity, thereby enabling the assembly and co-ordination of cell movements in the large vanguard rafts at the leading edge and in the smaller "bulldozer" aggregates that forge the interconnected furrow network. Interestingly tfp binding to the polysaccharide component of surface fibrils is proposed to act like a flexible fishing net that binds cells together in the leading edge rafts of *M. xanthus* cells during S motility mediated swarming (6). As *P. aeruginosa* tfp bind DNA (31), we propose that tfp-eDNA interactions may serve a similar function in *P. aeruginosa* biofilms by interconnecting cells to one another in a manner similar to the exopolysaccharide fibril net of *M. xanthus*.

In the presence of DNaseI we observed that cells displayed a lack of collective behaviour, resulting in traffic jams of misaligned cells. Interestingly, AFM analysis revealed that the presence of DNaseI resulted in deep, broad furrows with steep inclines to the surface. This suggests that continuous coordinated behaviour is required for cells to navigate within the furrow network, providing a constant stream of cells into the advancing rafts to ensure efficient migration of these structures across the surface and the resulting construction of the furrow network. Thus it is apparent that cellular alignment imposed by eDNA facilitates this mass transit of cells through the furrow network thereby avoiding traffic jams and ensuring an efficient supply of cells to the migrating front. Our analyses reveal that eDNA also co-ordinates the movements of cells in the leading edge vanguard rafts and is required for the assembly of cells into the "bulldozer" aggregates that forge the interconnecting furrows. Our observations have revealed that large-scale self-organization of cells in actively expanding biofilms of *P. aeruginosa* occurs through construction of an intricate network of furrows that is facilitated by eDNA.

Materials and Methods

Biofilm expansion assays. Colony biofilms were cultured at 37°C in humid conditions on 1xLB-Lennox solidified with either 1% agar (LBA) or 8g/L gellan gum (LBGG). Interstitial biofilms were cultured on 0.4xLB-Lennox solidified with 8g/L gellan gum (TMGG). Molten TMGG was poured over sterile slides and solidified at room temperature. Slides were inoculated, covered with a sterile coverslip and incubated in humid conditions at 37°C. Media was supplemented with 100 Kunitz units/mL DNaseI (D5025, Sigma Aldrich) or the enzyme storage buffer (50% glycerol, 10mM $MgCl_2$, 10mM $CaCl_2$, 10mM Tris-HCl). To visualise eDNA, TMGG was supplemented with the cell impermeant DNA stain TOTO-1 (1 or 2 μM; Life Technologies Corp.). For measurement of cell widths by OMX 3D-SIM, TMGG was supplemented with the membrane stain FM1-43FX (5μg/mL; Life Technologies Corp.)

Segmentation and tracking of bacteria. Individual bacteria across 100 s of high resolution phase-contrast microscopy time-series captured at 1 frame/2 s were identified by segmentation as described previously (23, 24). See Supplementary Information for description of quantitative analyses used in this study.

Atomic Force Microscopy. The topography of the media from washed interstitial biofilms was determined using an MFP-3D instrument (Asylum Research). Height images were collected using AC mode in air, with minimized loading force. Antimony (n) doped silicon cantilevers (Veeco TESP-SS) with a nominal spring constant of 42 N/m and a nominal probe curvature radius of 2 nm were used. A scan size of 60x60 μm was used which was large enough to differentiate between different regions of the biofilms. Tapping mode images were

processed and analysed using MFP-3D AFM (Asylum Research) or Image SXM (University of Liverpool) software.

Acknowledgments

CBW was supported by an Australian National Health and Medical Research Council Senior Research Fellowship (571905). LT was supported by a UTS Chancellor's Postdoctoral Fellowship.

Footnotes

Author Contributions

ESG, LT, HW, LGM, RC, SRO, LMN, MLG, IGC and CBW designed, performed and analysed experiments; PV generated cell tracking data; ESG, AH, MPW, LM, CH, JL, RP and CBW developed analytical tools and analysed cell tracking data; CBW conceived of and supervised the project. ESG and CBW and wrote the paper. All authors discussed the results and implications and commented on the manuscript. ESG and LT contributed equally to this work.

References

1. Donlan RM (2002) Biofilms: microbial life on surfaces. *Emerg Infect Dis* 8:881-890.
2. Donlan RM, Costerton JW (2002) Biofilms: survival mechanisms of clinically relevant microorganisms. *Clin Microbiol Rev* 15:167-193.
3. Sabbuba N, Hughes G, Stickler DJ (2002) The migration of *Proteus mirabilis* and other urinary tract pathogens over Foley catheters. *BJU Internat* 89:55-60.
4. Mauriello EMF, Mignot T, Yang ZM, Zusman DR (2010) Gliding motility revisited: How do the Myxobacteria move without flagella? *Microbiol. Mol. Biol. Rev.* 74:229-249.
5. Zhang Y, Ducret A, Shaevitz J, Mignot T (2012) From individual cell motility to collective behaviors: insights from a prokaryote, *Myxococcus xanthus*. *FEMS Microbiol Rev* 36:149-164.
6. Wu Y, Jiang Y, Kaiser D, Alber M (2007) Social interactions in myxobacterial swarming. *PLoS Comput Biol* 3(12):e253.
7. Wu Y, Kaiser AD, Jiang Y, Alber MS (2009) Periodic reversal of direction allows Myxobacteria to swarm. *Proc Natl Acad Sci USA* 106:1222-1227.
8. Harvey CW*, et al.* (2011) Study of elastic collisions of *Myxococcus xanthus* in swarms. *Phys Biol* 8:026016.
9. Holmes AB, Kalvala S, Whitworth DE (2010) Spatial simulations of myxobacterial development. *PLoS Comput Biol* 6(2):e1000686.
10. Henrichsen J (1983) Twitching motility. *Ann Rev Microbiol* 37:81-93.
11. Merz AJ, So M, Sheetz MP (2000) Pilus retraction powers bacterial twitching motility. *Nature* 407:98-102.
12. Skerker JM, Berg HC (2001) Direct observation of extension and retraction of type IV pili. *Proc Natl Acad Sci USA* 98:6901-6904.
13. Semmler AB, Whitchurch CB, Mattick JS (1999) A re-examination of twitching motility in *Pseudomonas aeruginosa*. *Microbiol* 145:2863-2873.
14. Vicsek T, Zafeiris A (2012) Collective motion. *Physics Reports* 517:71-140.
15. Boissard E, Degond P, Motsch S (2012) Trail formation based on directed pheromone depostition. *J. Math. Biol.* DOI: 10.1007/s00285-012-0529-6
16. Levine H, Ben-Jacob E (2004) Physical schemata underlying biological pattern formation-examples, issues and strategies. *Physical biology* 1:P14-22.
17. Grammaticos B, Badoual M, Aubert M (2007) An (almost) solvable model for bacterial pattern formation. *Physica D* 234:90-97.
18. Shapiro JA (1998) Thinking about bacterial populations as multicellular organisms. *Ann Rev Microbiol* 52:81-104.
19. Beatson SA, Whitchurch CB, Semmler AB, Mattick JS (2002) Quorum sensing is not required for twitching motility in *Pseudomonas aeruginosa*. *J Bacteriol* 184:3598-3604.
20. Burchard RP (1982) Trail following by gliding bacteria. *J. Bacteriol.* 152:495-501.
21. Stahl SJ, Stewart KR, Williams FD (1983) Extracellular slime associated with *Proteus mirabilis* during swarming. *J Bacteriol* 154:930-937.
22. Li YN*, et al.* (2003) Extracellular polysaccharides mediate pilus retraction during social motility of *Myxococcus xanthus*. *Proc Natl Acad Sci USA* 100:5443-5448.
23. Vallotton P, Mililli L, Turnbull L, Whitchurch CB (2010) Segmentation of dense 2D bacilli populations. in *International Conference on Digital Image Computing: Techniques and Applications (DICTA)* (Sydney), DOI: 10.1109/DICTA.2010.23.

24. Vallotton P, *et al.* (2009) Segmentation and tracking of individual *Pseudomonas aeruginosa* bacteria in dense populations of motile cells. in *Image and Vision Computing New Zealand 2009,* DOI: 10.1109/IVCNZ.2009.5378409.

25. Kaiser D, Warrick H (2011) *Myxococcus xanthus* swarms are driven by growth and regulated by a pacemaker. *J Bacteriol* 193:5898-5904.

26. Murakawa T (1973) Slime production by *Pseudomonas aeruginosa*. IV. Chemical analysis of two varieties of slime produced by *Pseudomonas aeruginosa*. *Jpn J Microbiol* 17:513-520.

27. Matsukawa M, Greenberg EP (2004) Putative exopolysaccharide synthesis genes influence *Pseudomonas aeruginosa* biofilm development. *J Bacteriol* 186:4449-4456.

28. Steinberger RE, Holden PA (2004) Macromolecular composition of unsaturated *Pseudomonas aeruginosa* biofilms with time and carbon source. *Biofilms* 1:37-47.

29. Allesen-Holm M, *et al.* (2006) A characterization of DNA release in *Pseudomonas aeruginosa* cultures and biofilms. *Mol Microbiol* 59:1114-1128.

30. Whitchurch CB, Tolker-Nielsen T, Ragas PC, Mattick JS (2002) Extracellular DNA required for bacterial biofilm formation. *Science* 295:1487.

31. van Schaik EJ, *et al.* (2005) DNA binding: a novel function of *Pseudomonas aeruginosa* type IV pili. *J Bacteriol* 187:1455-1464.

32. Bakaletz LO, *et al.* (2005) Demonstration of Type IV pilus expression and a twitching phenotype by *Haemophilus influenzae*. *Infect Immun* 73:1635-1643.

33. Eijkelkamp BA, *et al.* (2011) Adherence and motility characteristics of clinical *Acinetobacter baumannii* isolates. *FEMS Microbiol Lett* 323:44-51.

34. Narayan V, Menon N, Ramaswamy S (2006) Nonequilibrium steady states in a vibrated-rod monolayer: tetratic, nematic, and smectic correlations. *J Stat Mech-Theor Expt*:P01005.

35. Smalyukh, II, Butler J, Shrout JD, Parsek MR, Wong GC (2008) Elasticity-mediated nematiclike bacterial organization in model extracellular DNA matrix. *Physic Rev E, Stat Nonlin Soft Matt Phys* 78:030701.

Figure Legends

Figure 1. Tracking of cellular movements during interstitial biofilm expansion. Time-series (1 frame/2 s) of interstitial biofilm expansion of *P. aeruginosa* strain PAK cultured on TMGG in the absence and presence of DNaseI (Video S1, S5). Regions at the leading edge of the expanding biofilms (**A, E**; Video S1, S5) and behind the leading edge (**C**, **G**; Video S1, S5) were imaged with phase contrast microscopy. Panels **(A**, **C**, **E**, **G)** correspond to the first image of each time-series. Scale bar 20 μm. Every cell present throughout the first 50 frames of each time-series was tracked and the paths traversed by each cell represented graphically (**B**, **D**, **F**, **H**). Tick distance 10 μm. Arrows indicate overall direction of movement away from the main biofilm toward unoccupied territory. Boxed regions (**A**, **E**) indicate cells in

regions designated “Raft head” whilst the remainder of the cells in the field of view were designated as “Raft trails” for the quantitative analyses of cell movements.

Figure 2. Quantitative analyses of cell tracking data. (A) Velocity coherence across 50 frames of each cells with its closest neighbors in the indicated regions of the biofilm in the absence (open circle) and presence (black circle) of DNaseI. Each point indicates mean velocity coherence for all cells in a given frame. Error bars are ± sem. Total distances **(B)** and net displacements **(C)** over 100 s of individual cells in the indicated regions of interstitial biofilms grown in the absence (-; white box) and presence (+; grey box) of DNaseI. **(D)** Autocorrelations of velocity direction in the indicated regions of the biofilm in the absence (open circle) and presence (black circle) of DNaseI. Each point indicates mean velocity direction autocorrelations for all cells in a given frame. Error bars are ± sem. *** indicates p-value <0.001, ** p-value <0.01 and * < 0.05 for comparisons of data sets obtained in the absence of DNaseI with corresponding data sets obtained in the presence of DNaseI.

Figure 3. Interstitial biofilm trails are furrows. (A) Phase contrast image of the leading edge of a colony biofilm of wildtype *P. aeruginosa* strain PA103 cultured on LBGG showing the phase bright trails (white arrow) produced in the wake of the advancing rafts. Scale bar 50 μm. Phase-contrast image of a *P. aeruginosa* PAK interstitial biofilm cultured on TMGG **(B)** and the corresponding phase-contrast image of the underlying substrate showing phase bright trails **(C)**. **(D)** Overlay of panels **(B, C)**. Scale bar 30 μm. 3D rendered images of AFM measurements taken from washed interstitial biofilm substrate at the leading edge **(E)** and trail network **(F)**. **(G)** Phase-contrast images of the assembly of a small “bulldozer” aggregate breaking away from an established trail in an interstitial biofilm to form a new trail that intersects with another newly formed trail (see Video S3). Scale bar 5 μm. Time indicated

taken from the start of the time series.

Figure 4. Interstitial biofilms contain eDNA. Interstitial biofilms of PAK containing pUCP*cfp* (blue) cultured on TMGG containing the eDNA stain TOTO-1 (yellow) and imaged using OMX-Blaze^{TM} showing eDNA is present in the leading edge rafts (**A, B**), and in the trail network (**C, D**). (**B**) and (**D**) are the TOTO-1 channels of (**A**) and (**C**) respectively. (**E**) shows alignment of bacteria and strands of eDNA as it is spread throughout the biofilm by cellular movement. **(A)** and **(B)** were obtained with TMGG supplemented with 2μm TOTO-1 and panels **(C)**, **(D)** and **(E)** were obtained with TMGG supplemented with1 μm TOTO-1. The contrast in the TOTO-1 channel was set to enable visualization of low intensity eDNA staining. Scale bar 5 μm. **(F)** Phase-contrast images of underlying nutrient media that supported an interstitial biofilm of *P. aeruginosa* strain PAK cultured on TMGG in the presence of DNaseI. **(G)** Overlay of the trails depicted in **(F)** with the corresponding phase-contrast image of the intact interstitial biofilm. Scale bar 30 μm. 3D rendered images of AFM measurements taken from washed interstitial biofilm substrate in the presence of DNaseI at the leading edge **(H**) and behind the leading edge **(I**).

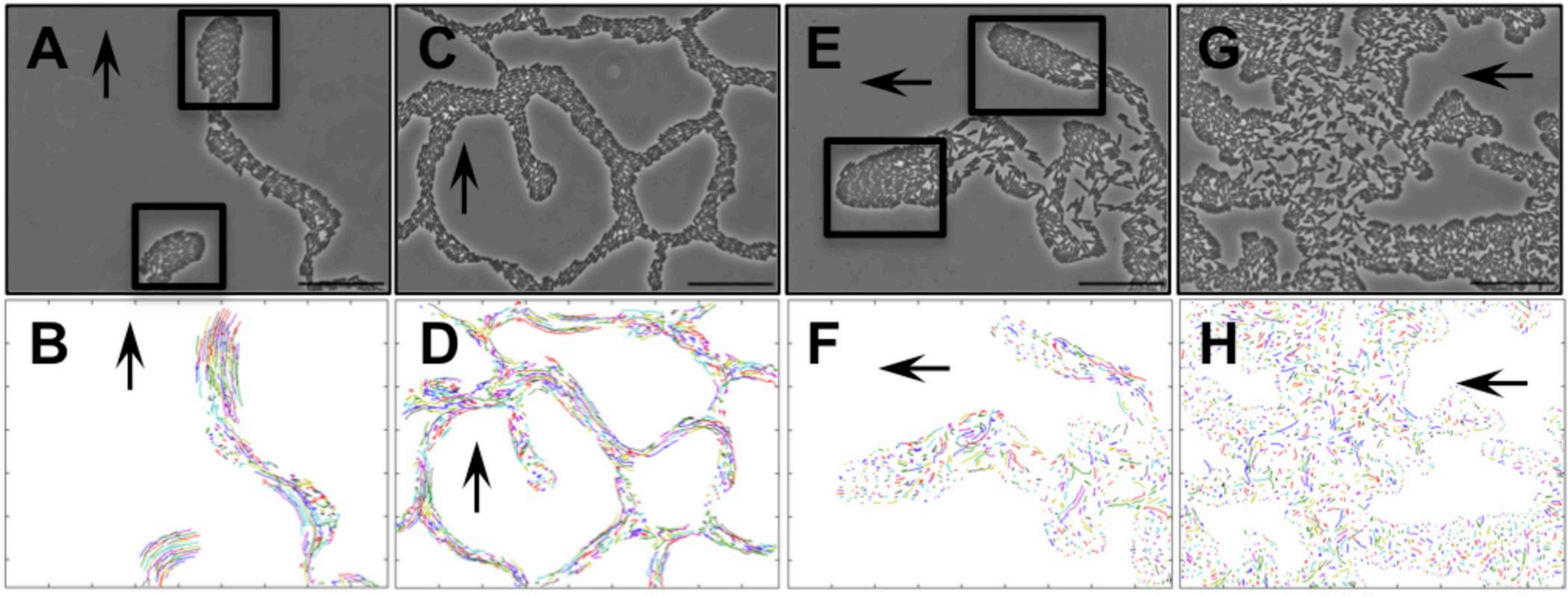
A
C
E
G
B
D
F
H

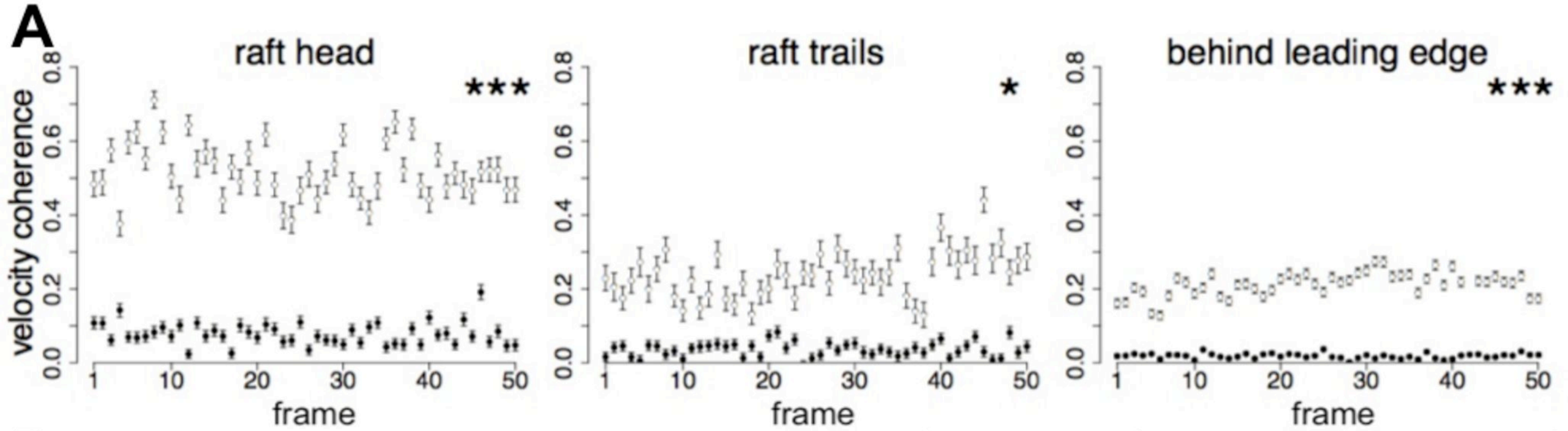
A
raft head
raft trails
behind leading edge
***
*
***
velocity coherence
0.0
0.2
0.4
0.6
0.8
1
10
20
30
40
50
frame

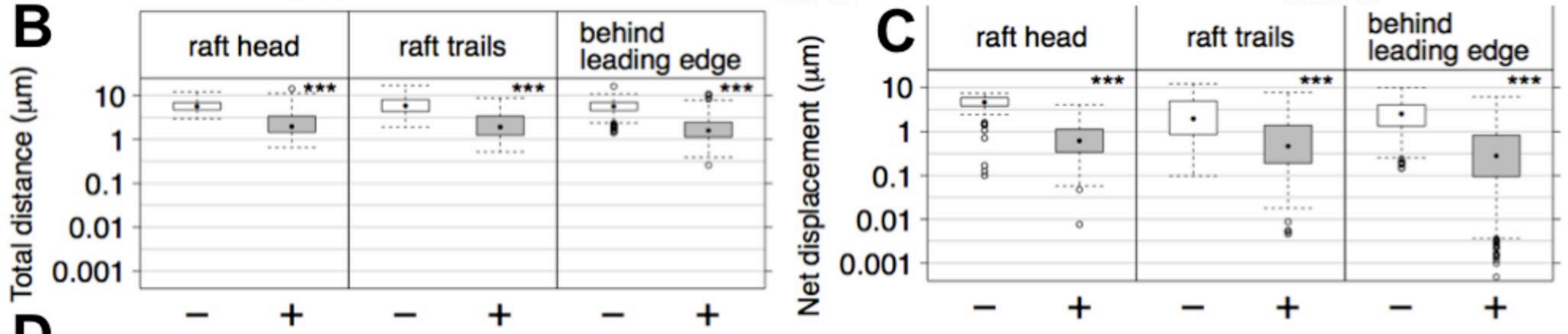
B
raft head
raft trails
behind leading edge
***
Total distance (μm)
10
1
0.1
0.01
0.001
−
+

C
raft head
raft trails
behind leading edge
***
Net displacement (μm)
10
1
0.1
0.01
0.001
−
+

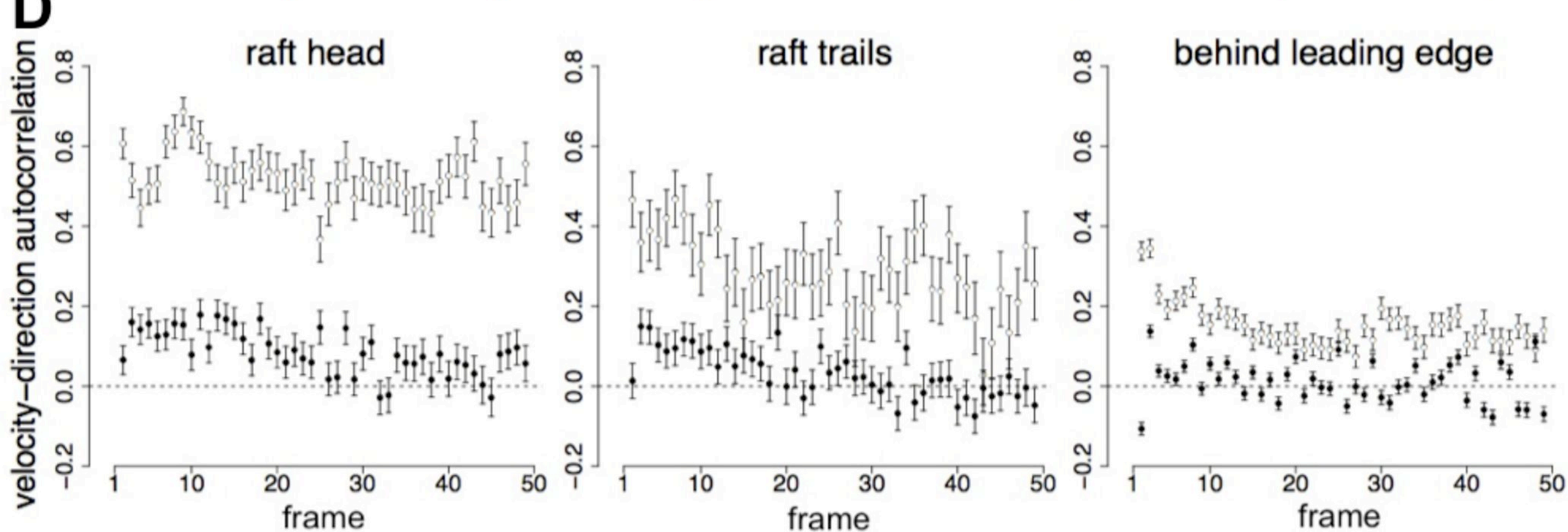
D
raft head
raft trails
behind leading edge
velocity−direction autocorrelation
0.8
0.6
0.4
0.2
0.0
−0.2
1
10
20
30
40
50
frame